

Anisotropies in the Motions and Positions of the Galactic Globular Clusters

F.D.A. Hartwick

Department of Physics and Astronomy,
University of Victoria, Victoria, BC, Canada, V8W 3P6

ABSTRACT

The velocity ellipsoid for 38 globular clusters with $[\text{Fe}/\text{H}] \leq -1.0$ is derived and shown to be significantly anisotropic with major axis directed towards low Galactic latitude. Principal axes of the spatial distribution of different groups of clusters are derived and compared with the velocity ellipsoid. The metal poor cluster spatial distribution is significantly flattened along an axis which coincides within the uncertainties with the major axis of the velocity ellipsoid. Given the observed steep age-metallicity relation for metal poor clusters, one speculative interpretation of the data is that an initially flattened filament underwent a relatively rapid initial transverse collapse forming satellite galaxies and metal poor globular clusters while the protogalaxy collapsed and assembled more slowly along the filament acquiring and/or redistributing angular momentum in the process.

Subject headings: Galaxy: halo — Galaxy: formation — globular clusters: general

1. Introduction

Globular clusters provide a unique probe of the earliest phases of the evolution of the Galaxy. From the early work of Kinman (1959), Zinn (1985), and others it is clear that the clusters can be divided into at least two groups – the spatially extended, metal poor blue clusters and the more centrally concentrated towards the Galactic center, metal rich red clusters. This work is concerned primarily with the former group, and the main motivation is the recent availability of space motions for a significant number of these clusters as published by Dinescu et al. (1999). Dinescu (private communication) has also provided this author with data for 4 additional clusters. These data are used to determine the velocity ellipsoid for the metal poor group in order to allow a comparison with the

spatial distribution. In a previous paper (Hartwick 2000, hereafter H2000) the spatial distribution of various halo samples was examined. There it was found that the metal poor group of globular clusters formed an oblate distribution whose minor axis was directed to a low Galactic latitude. This was in contrast to the metal rich group which exhibited a triaxial distribution with minor axis toward the Galactic pole. We re-examine the spatial distributions with modified samples of clusters and compare the results with the kinematics.

2. The Velocity Dispersion Tensor of the Halo Clusters

Danescu et al. (1999) have compiled space motions for 38 globular clusters, and 35 of these have $[\text{Fe}/\text{H}]$ values less than -1.0 . Since that time 3 more halo clusters (NGC6522, NGC7006, & Pal 13) have been added to the compilation. This sample of 38 clusters is the basis for the following kinematical investigation. The tabulated UVW components of space motion (corrected solar peculiar motion and for Galactic rotation of 220 km sec^{-1}) are referred to the Galactic center where V_π is the radial component in the Galactic plane directed positive away from the center, V_ϕ is the tangential component positive in the direction of Galactic rotation and V_z is the vertical component directed positive in the direction of the north Galactic pole.

The average of each of these components for the entire sample was removed before forming the following six moments: $\overline{V_\pi V_\pi}$, $\overline{V_\phi V_\phi}$, $\overline{V_z V_z}$, $\overline{V_\pi V_\phi}$, $\overline{V_\pi V_z}$, and $\overline{V_\phi V_z}$. These six moments are the components of the symmetrical velocity dispersion tensor. The eigenvalues of the matrix were then determined in the standard way and are given below. The units of the eigenvalues denoted by σ are km sec^{-1} and the one sigma uncertainties throughout were computed by the bootstrap method.

$$\begin{aligned}
 & \text{Clusters with } [\text{Fe}/\text{H}] < -1.00 \text{ (n=38)} \\
 \sigma_a &= 161_{-15.0}^{+18.3} & l &= 338_{-6.65}^{+10.5} & b &= -5.65_{-15.0}^{+13.6} \\
 \sigma_b &= 120_{-15.5}^{+9.44} & l &= 87.2_{-30.0}^{+155.} & b &= -73.5_{-6.63}^{+27.9} \\
 \sigma_c &= 95.6_{-17.6}^{+2.66} & l &= 66.1_{-10.8}^{+11.2} & b &= 15.4_{-21.1}^{+22.2} \\
 & & \overline{V_\phi} &= 59.6_{-17.9}^{+13.5}
 \end{aligned} \tag{1}$$

As a check on the sensitivity of the above result to the $[\text{Fe}/\text{H}]$ cutoff, we repeated the procedure for the 26 clusters with $[\text{Fe}/\text{H}] < -1.5$ and find:

$$\text{Clusters with } [\text{Fe}/\text{H}] < -1.50 \text{ (n=26)}$$

$$\begin{aligned}
 \sigma_a &= 172_{-19.2}^{+17.9} & l &= 330_{-8.11}^{+11.4} & b &= -6.31_{-14.5}^{+14.9} \\
 \sigma_b &= 122_{-27.7}^{+8.45} & l &= 179_{-112}^{+91.7} & b &= -82.8_{+6.58}^{+32.6} \\
 \sigma_c &= 94.7_{-27.8}^{+5.76} & l &= 60.8_{-12.1}^{+12.1} & b &= -3.48_{-21.3}^{+30.1} \\
 \overline{V_\phi} &= 49.3_{-28.1}^{+23.7}
 \end{aligned} \tag{2}$$

In both of the above solutions the mean streaming motions in the π and z directions differed from zero by less than 1.5 sigma. Also the above values of $\overline{V_\phi}$ are independent of distance from the Galactic center.

Asymmetric error ellipsoids in the components of space motion can be expected due to relatively small errors in radial velocity and relatively large errors in proper motion. In order to ensure that such effects were not unduly influencing solution (1) the errors in radial velocity, proper motion and distance given by Dinescu et al. (1999) were used as dispersions in assumed gaussian distributions and solutions were performed on space motions determined by the propagation of randomly chosen uncertainties in each of the above quantities. The mean and standard deviation of the major axis from 100 trials with 38 clusters is $\sigma_a = 167 \pm 7.98$ towards $l = 332 \pm 6.28$ and $b = -5.94 \pm 7.64$. Results for the other two axes are $\sigma_b = 122 \pm 10.9$ and $\sigma_c = 108 \pm 10.1$. This independent assessment of uncertainties thus strengthens the case for the generally *prolate* velocity ellipsoid given by solution (1).

An examination of the spatial distribution of the clusters from solution (1) shows that only 7 of the 38 clusters were in the hemisphere beyond the Galactic center. In order to assess the effect of this spatial imbalance on our result, kinematic solutions were made using the above 7 clusters combined with 7 independently chosen clusters from the hemisphere containing the sun. Thirty solutions were made with 14 clusters each and the median results for each aspect of the major axis are: $\sigma_a = 166_{-9}^{+20}$, $l = 348_{-7}^{+8}$, and $b = -13_{-8}^{+29}$. While the one sigma uncertainties of solution (1) do overlap with the above result, perhaps the most important implication of this exercise is a clear need for more cluster space motion determinations.

3. The Spatial Distribution of the Globular Clusters

The spatial distribution of the outlying satellites and the globular clusters was determined in H2000. There it was found that the 99 metal poor globular clusters ($[\text{Fe}/\text{H}] \leq -1.0$) formed an oblate distribution with minor axis directed towards $l = 307^\circ, b = -3.3^\circ$ quite different from the short axis of the distribution of the satellite galaxies. The result from the kinematics described above prompted a re-examination of this

result. It is believed that the pole of the orbit of the Sagittarius system is highly inclined to that of the remaining outlying satellite galaxies (Lynden-Bell & Lynden-Bell 1995). As well these authors tentatively assign the 6 clusters M54, NGC2419, Arp 2, Pal 2, Terzan 7 and Terzan 8 to the Sagittarius stream. Given that the present orbit of Sagittarius is probably not the one that it had at formation (c.f. Zhao 1998, also Johnston et al. 2002) we removed the above clusters from the original sample and performed new solutions. (Note that the Harris (1996) web-based compilation contains 147 clusters of which 99 have $[\text{Fe}/\text{H}] \leq -1.0$. Culling 5 clusters from this sub-group still leaves us with 95% of the original sample. Furthermore, none of these five clusters was included in the above kinematic solutions.) The analysis procedure followed here is slightly different from that in H2000. Here the tensor components $\overline{x_i x_i}, \overline{x_i y_i}$ etc were calculated both without weighting and with weighting by $1/d_i$ where the $x_i, y_i,$ and z_i are the projections of d_i , the distance from the Galactic center ($R_0 = 8$ kpc assumed). Both the weighted and unweighted solutions are given since the true distribution probably lies somewhere in between. The eigenvalues of the resulting matrix are denoted $e_a, e_b,$ and e_c and have units of kpc.

Cluster Sample with $[\text{Fe}/\text{H}] \leq -1.0$ (weighted) (n=94)

$$\begin{aligned}
 e_a &= 5.30^{+1.77}_{-1.11} & l &= 246^{+33.6}_{-11.1} & b &= -40.0^{+24.0}_{-18.2} \\
 e_b &= 5.04^{+1.31}_{-0.742} & l &= 44.1^{+19.2}_{-12.1} & b &= 48.0^{+12.4}_{-28.3} \\
 e_c &= 3.22^{+0.241}_{-0.464} & l &= 326^{+13.9}_{-12.2} & b &= -10.8^{+7.22}_{-13.5} \\
 c/a &= 0.61^{+0.13}_{-0.14}
 \end{aligned} \tag{3}$$

Cluster Sample with $[\text{Fe}/\text{H}] \leq -1.0$ (unweighted) (n=94)

$$\begin{aligned}
 e_a &= 19.9^{+4.03}_{-5.32} & l &= 236^{+8.20}_{-24.8} & b &= -63.2^{+25.6}_{-11.6} \\
 e_b &= 15.5^{+2.90}_{-5.25} & l &= 52.3^{+21.3}_{-8.04} & b &= -26.8^{+15.8}_{-22.6} \\
 e_c &= 8.18^{+0.306}_{-2.01} & l &= 323^{+11.7}_{-9.19} & b &= 1.53^{+4.06}_{-18.6} \\
 c/a &= 0.41^{+0.093}_{-0.091}
 \end{aligned} \tag{4}$$

As a check on the robustness of the result, solutions were also made for the 60 remaining clusters with $[\text{Fe}/\text{H}] \leq -1.5$.

Cluster Sample with $[\text{Fe}/\text{H}] \leq -1.5$ (weighted) (n=60)

$$\begin{aligned}
 e_a &= 5.76^{+1.66}_{-0.721} & l &= 115^{+66.3}_{-36.5} & b &= -61.3^{+24.2}_{-4.81} \\
 e_b &= 5.34^{+1.57}_{-1.07} & l &= 60.2^{+22.9}_{-20.0} & b &= 17.3^{+29.0}_{-23.2} \\
 e_c &= 3.67^{+0.249}_{-0.511} & l &= 337^{+10.6}_{-39.4} & b &= -22.1^{+12.7}_{-10.3} \\
 c/a &= 0.64^{+0.061}_{-0.15}
 \end{aligned} \tag{5}$$

Cluster Sample with $[\text{Fe}/\text{H}] \leq -1.5$ (unweighted) (n=60)

$$\begin{aligned}
 e_a &= 19.4^{+4.67}_{-7.93} & l &= 238^{+10.0}_{-33.8} & b &= -48.5^{+10.8}_{-2.93} \\
 e_b &= 15.1^{+4.12}_{-5.89} & l &= 66.2^{+31.9}_{-8.99} & b &= -41.3^{+11.8}_{-3.54} \\
 e_c &= 8.29^{+0.112}_{-2.11} & l &= 333^{+18.2}_{-27.5} & b &= -3.90^{+8.86}_{-23.0} \\
 c/a &= 0.43^{+0.13}_{-0.11}
 \end{aligned} \tag{6}$$

We note that for both samples the short axis of the (nearly oblate) cluster distribution is very similar to the *long* axis of the kinematic solution. In order to insure that our result is not affected by incompleteness or uncertain absorption corrections, solutions were also performed for only those clusters whose absolute Galactic latitudes were larger than 10° .

Cluster Sample with $[\text{Fe}/\text{H}] \leq -1.0$ and $|b| > 10$ (weighted) (n=66)

$$\begin{aligned}
 e_a &= 7.93^{+2.32}_{-0.618} & l &= 192^{+54.2}_{-76.1} & b &= -76.4^{+33.2}_{+0.863} \\
 e_b &= 7.11^{+0.568}_{-1.55} & l &= 58.6^{+21.9}_{-11.9} & b &= -9.44^{+29.4}_{-33.0} \\
 e_c &= 4.64^{+0.268}_{-0.591} & l &= 327^{+14.4}_{-11.3} & b &= -9.65^{+6.99}_{-12.6} \\
 c/a &= 0.58^{+0.011}_{-0.13}
 \end{aligned} \tag{7}$$

Cluster Sample with $[\text{Fe}/\text{H}] \leq -1.0$ and $|b| > 10$ (unweighted) (n=66)

$$\begin{aligned}
 e_a &= 23.6^{+6.37}_{-6.36} & l &= 236^{+34.1}_{-20.1} & b &= -65.1^{+22.1}_{-7.44} \\
 e_b &= 17.8^{+2.33}_{-4.45} & l &= 50.3^{+15.3}_{-10.7} & b &= -24.8^{+21.1}_{-20.0} \\
 e_c &= 9.43^{+0.372}_{-1.97} & l &= 321^{+9.03}_{-9.78} & b &= 2.05^{+6.38}_{-11.1} \\
 c/a &= 0.40^{+0.071}_{-0.092}
 \end{aligned} \tag{8}$$

The quoted uncertainties in the above solutions were determined by the bootstrap method. It is instructive to consider the effects on the solution of errors in the individual distances to each cluster. Randomly chosen errors drawn from a gaussian distribution with a sigma of 10% of each distance were propagated through and the mean and standard deviation of the minor axis of the spatial distribution from 100 trials with 66 clusters was found to be $e_c = 4.67 \pm 0.0949$ towards $l = 327 \pm 1.28$ and $b = -9.91 \pm 1.02$. The amplitudes of the other two axes are $e_a = 7.98 \pm 0.146$ and $e_b = 7.11 \pm 0.148$. The good agreement with solution (7) strengthens the case for the generally *oblate* spatial distribution given by solution (7).

For illustration, the distribution of clusters in this new coordinate system (solution (7)) is shown in Fig. 1 where x' are projections of Galactocentric distance along the major axis

and z' are projections along the minor axis. As summarized in Table 1, the short axes of the spatial distributions are remarkably similar to the major axes of the kinematic solutions of the previous section. Furthermore, the minor axis of the satellite galaxy distribution is also quite similar.

In H2000 the spatial distribution of the 34 most metal rich globular clusters ($[\text{Fe}/\text{H}] \geq -0.7$) was also determined. The distribution was found to be triaxial with the long axis directed slightly off ($\sim 17^\circ$) the sun-center line and the short axis now pointing to high Galactic latitude. We repeat the process below but with one less cluster (Terzan 7).

$$\begin{aligned}
 &\text{Cluster Sample with } [\text{Fe}/\text{H}] \geq -0.7 \text{ (weighted) (n=33)} \\
 &e_a = 2.02^{+0.431}_{-0.251} \quad l = 338^{+6.19}_{-29.0} \quad b = -6.09^{+4.63}_{-2.92} \\
 &e_b = 1.51^{+0.273}_{-0.228} \quad l = 68.1^{+14.5}_{-12.7} \quad b = 0.430^{+9.99}_{-9.13} \\
 &e_c = 0.761^{+0.0968}_{-0.174} \quad l = 334^{+65.2}_{-60.2} \quad b = 83.9^{+0.907}_{-9.95} \\
 &c/a = 0.38^{+0.049}_{-0.094}
 \end{aligned} \tag{9}$$

$$\begin{aligned}
 &\text{Cluster Sample with } [\text{Fe}/\text{H}] \geq -0.7 \text{ (unweighted) (n=33)} \\
 &e_a = 3.78^{+1.00}_{-1.29} \quad l = 335^{+4.86}_{-11.9} \quad b = -8.50^{+7.51}_{-2.76} \\
 &e_b = 2.29^{+0.336}_{-0.472} \quad l = 65.7^{+6.05}_{-9.34} \quad b = -3.51^{+12.9}_{-10.1} \\
 &e_c = 1.11^{+0.0711}_{-0.413} \quad l = 358^{+37.5}_{-85.6} \quad b = -80.8^{+0.623}_{-9.86} \\
 &c/a = 0.29^{+0.088}_{-0.12}
 \end{aligned} \tag{10}$$

A triaxial distribution is still present, but now the major axis is $\sim 26^\circ$ off of the sun-center line while the minor axis is directed to high latitude. Again it seems reasonable to suggest that we are observing a globular cluster counterpart to the ‘COBE’ bar (c.f. Binney & Merrifield, 1998, p. 616). Should future work confirm the remarkably close alignment between the major axis of the spatial distribution and the major kinematic dispersion axis (see Table 1), an intimate connection between halo (metal poor clusters) and bulge (metal rich clusters) would be implied. One possible argument against such a connection is the recent suggestion that bars may be less common at high redshift than at $z=0$ (van den Bergh et al. 2002). Further elucidation will come from the determination of the space motions for these metal rich clusters.

4. Discussion

Both the velocity ellipsoid and the spatial distribution of the most metal poor Galactic globular clusters appear to be anisotropic. It is interesting that the major axis of the

velocity ellipsoid is directed towards low Galactic latitude, consistent with the direction of the short axis of the spatial distribution and not far from the pole of the outlying satellite galaxy distribution. A quantitative comparison for the different samples is given in Table 1 where for reference we take the major axis of the kinematic solution (1).

There would appear to be no straight forward explanation for the observations above. If the gravitational potential was spherical, one can argue that the direction of highest velocity dispersion would also be that of the longest spatial axis and vice versa. The above result then apparently rules out a spherical potential but would be consistent with one that was flattened in the direction of highest velocity dispersion. Recalling that the age-metallicity relation for the most metal poor globular clusters is extremely steep (vandenBerg 2000), a naive picture is that an initially flattened filament underwent a rapid collapse transverse to the long axis during which time satellite galaxies, the metal poor clusters, and the triaxial structure discussed in H2000 were formed. Simultaneously the Galaxy was being assembled by a slower collapse along the filament during which time most of its angular momentum was being induced and/or redistributed. While triaxial structures are formed in cold dark matter simulations, the scenario outlined above may be more consistent with a warm dark matter theory for structure formation where the lowest mass objects form from the fragmentation of caustics (c.f. Bode, Ostriker, & Turok 2001).

The author wishes to thank Dr. Dana Dinescu for providing the latest compilation of cluster space motions in convenient form, and Ray Carlberg, Scott Tremaine, and Sidney van den Bergh for their helpful comments on an earlier draft. He also wishes to acknowledge financial support from an NSERC of Canada operating grant.

REFERENCES

- Binney, J., & Merrifield, M. 1998, *Galactic Astronomy*, (Princeton: PUP)
- Bode, P., Ostriker, J.P. & Turok, N. 2001, *ApJ*, 556, 93
- Dinescu, D.I., Girard, T.M., & van Altena, W.F. 1999, *AJ*, 117, 1792
- Harris, W.E. 1996, *AJ*, 112, 1487
- Hartwick, F.D.A. 2000, *AJ*, 119, 2248 (H2000)
- Johnston, K.V., Spergel, D.N., & Haydn, C. 2002, *ApJ*, 570, 656
- Kinman, T. D. 1959, *MNRAS*, 119, 538
- Lynden-Bell, D., & Lynden-Bell, R.M. 1995, *MNRAS*, 275, 429

Table 1. Comparison of the Axes of the Various Samples

Sample	Number n	Solution number	Axis Major/Minor	Galactic Coordinates		$\Delta\theta^a$
				l	b	
Velocity ellipsoid [Fe/H] ≤ -1.0	38	1	Major	$338^{+10.5}_{-6.65}$	$-5.65^{+13.6}_{-15.0}$	0°
Velocity ellipsoid [Fe/H] ≤ -1.5	26	2	Major	$330^{+11.4}_{-8.11}$	$-6.31^{+14.9}_{-14.5}$	$8.0^\circ \pm 13$
Clusters [Fe/H] ≤ -1.0	94	3	Minor	$326^{+13.9}_{-12.2}$	$-10.8^{+7.22}_{-13.5}$	$13^\circ \pm 16$
Clusters [Fe/H] ≤ -1.5	60	5	Minor	$337^{+10.6}_{-39.4}$	$-22.1^{+12.7}_{-10.3}$	$16^\circ \pm 18$
Clusters [Fe/H] ≤ -1.0 , $ b > 10^\circ$	66	7	Minor	$327^{+14.4}_{-11.3}$	$-9.65^{+6.99}_{-12.6}$	$11^\circ \pm 16$
Outlying Satellites	10	H2000	Minor	$336^{+8.28}_{-3.79}$	$11.1^{+3.89}_{-5.05}$	$17^\circ \pm 15$
Clusters [Fe/H] ≥ -0.7	33	9	Major	$338^{+6.19}_{-29.0}$	$-6.09^{+4.63}_{-2.92}$	$0.44^\circ \pm 15$

^a $\Delta\theta$ is the angular difference in degrees between axes of the first sample and each of the subsequent samples.

vandenBerg, D. A. 2000, ApJS, 129, 315

van den Bergh, S., Abraham, R.G., Whyte, L.F., Merrifield, M.R., Eskridge, P.B., Frogel,
J.A. & Pogge, R. 2002, AJ, 123, 2913

Zhao, H. 1998, ApJ, 500, L149

Zinn, R. 1985, ApJ, 293, 424

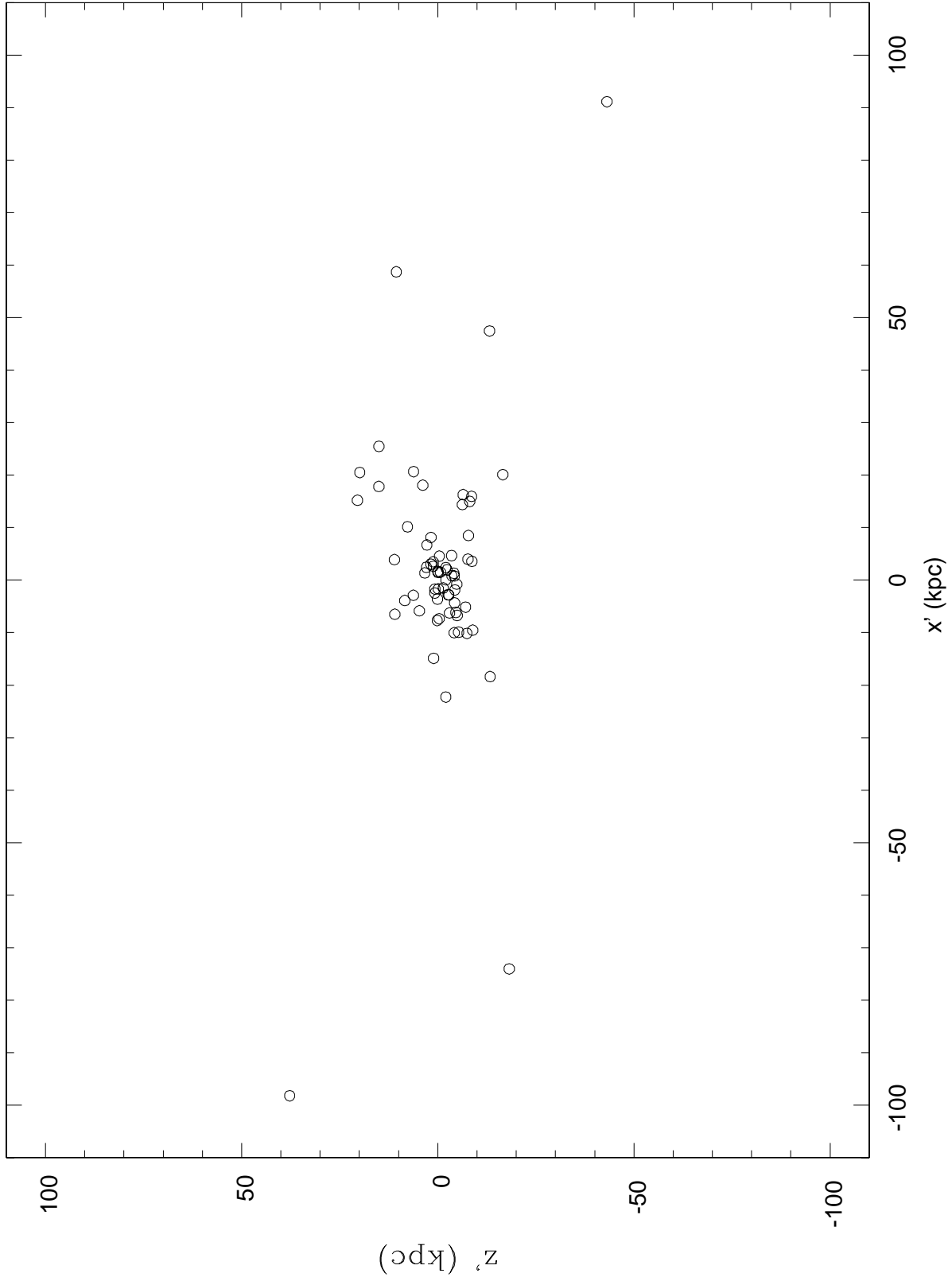


Fig. 1.— The spatial distribution of 66 globular clusters with $[\text{Fe}/\text{H}] \leq -1.0$ and $|b| > 10^\circ$ in coordinates transformed to the major (x') and minor (z') axes of solution (7) illustrating the flattening of the distribution. For reference the minor axis is directed to $l = 327^\circ$, $b = -9.65^\circ$.